Experimental study on super-resolution techniques for high-speed UWB radar imaging of human bodies

T. Sakamoto, H. Taki and T. Sato

Graduate School of Informatics, Kyoto University
Yoshida-Honmachi, Sakyo-ku, Kyoto, 606-8501 Japan

Abstract

UWB (Ultra Wide-Band) radar systems are used in a variety of applications. The UWB radar imaging algorithm SEABED (Shape Estimation Algorithm based on BST and Extraction of Directly scattered waves) is a method that can be used in real-time operation, although it requires high-resolution data. Although the resolution of radar is basically restricted by its bandwidth, super-resolution techniques can be used to overcome the conventional resolution limit. In this paper, we investigate super-resolution techniques for UWB radar experimental data.

1 Introduction

UWB radar systems are used in a variety of applications including land-mine detection, driving assistance and robotics. The fast UWB radar imaging algorithm SEABED [1], is, however, the only method that can be used in applications demanding real-time operation, such as security surveillance systems. The SEABED algorithm is based on a reversible transform IBST (Inverse Boundary Scattering Transform) between the target shape and a time delay observed at multiple locations. Because the IBST is very sensitive to the resolution of the time delay, it is imperative that high-resolution data be obtained to estimate various parts of the human-body. Although the resolution of radar is basically restricted by its bandwidth, super-resolution techniques have been applied to GPR (Ground Penetrating Radar) to enhance the conventional resolution limit [2]. In this paper, we investigate experimentally super-resolution techniques for UWB radar data using a pig's anterior abdominal wall as a model of the human body. The results show that the super-resolution techniques are indeed capable of improving the UWB radar performance.

2 SEABED Algorithm

We assume a mono-static radar system, in which an omni-directional antenna is scanned along a straight line. UWB pulses are transmitted at fixed intervals and received by the antenna. The received data is converted from analog to digital and stored in memory. We estimate target shapes using the obtained data. We define a real space in which targets and the antenna are located. We express the 2-dimensional real space with the parameters (x, y). Both x and y are normalized by λ, which is the center wavelength of the transmitted pulse in air. We assume $y > 0$ for simplicity. The antenna is scanned along the x-axis in r-space. We define $s(X, Y)$ as the received waveform after applying a matched filter at the antenna location $(x, y) = (X, 0)$. Here, we define Y with time t and the speed of the radiowave c as $Y = ct/(2\lambda)$. We define a data space expressed by (X, Y).

In previous work we developed a fast radar imaging algorithm, SEABED, based on a BST (Boundary Scattering Transform) [3, 4, 5, 6]. The algorithm uses a reversible transform, BST, between target shapes and pulse delays. The BST is expressed as

$$X = x + y \mathrm{d}y/\mathrm{d}x, \tag{1}$$

$$Y = y\sqrt{1 + (\mathrm{d}y/\mathrm{d}x)^2}, \tag{2}$$

where (X, Y) is a point on a quasi-wavefront, and (x, y) is a point on the target boundary [7]. The inverse transform of the BST is given by

$$x = X - Y \mathrm{d}Y/\mathrm{d}X, \qquad (3)$$

$$y = Y\sqrt{1 - (\mathrm{d}Y/\mathrm{d}X)^2}, \qquad (4)$$

where we assume $|\mathrm{d}Y/\mathrm{d}X| \leq 1$. This condition is required because y should be a real number. First, quasi-wavefronts are extracted from the received signals $s(X, Y)$ in the SEABED algorithm. Quasi-wavefronts are extracted to satisfy the conditions $\mathrm{d}s(X, Y)/\mathrm{d}Y = 0$ and $|\mathrm{d}Y/\mathrm{d}X| \leq 1$. Finally, we apply the IBST to the quasi-wavefronts, and obtain the final image. The extraction of quasi-wavefronts is critical to obtaining high-quality images with this algorithm. However, the quasi-wavefronts cannot be accurately estimated if multiple echoes are closely located in the received signal. Therefore, high-resolution techniques are indispensable to apply the SEABED algorithm in actual environments.

3 Frequency-Domain High-Resolution Method

The MUSIC (MUltiple SIgnal Classification) algorithm [8] is often used as a high-resolution imaging method for multiple signals based on the eigen-decomposition of correlation matrices. Suppose $g(t)$ is a transmitted signal and $G(\omega)$ is its Fourier transform, where ω is an angular frequency. Suppose $f_0(t)$ is a received signal and $F_0(\omega)$ is its Fourier transform. To retrieve the propagation transfer function, we apply the inverse filter to $F_0(\omega)$ as $F(\omega) = F_0(\omega)/G(\omega)$. Furthermore, suppose a vector $\boldsymbol{x}$ is defined as

$$\boldsymbol{x} = [F(\omega_1), F(\omega_2), \cdots, F(\omega_M)]^{\mathrm{T}}, \qquad (5)$$

where T denotes the transposition operator of a matrix. Let us introduce a correlation matrix $R_{xx} = \mathrm{E}[\boldsymbol{x}\boldsymbol{x}^{\mathrm{H}}]$, where E is the expectation operator, and H denotes the Hermite operator. Suppose R_{xx} has eigenvalues $\lambda_1 \geq \lambda_2 \geq \cdots \geq \lambda_M$ and corresponding eigenvectors $\boldsymbol{e}_1, \boldsymbol{e}_2, \cdots, \boldsymbol{e}_M$. Suppose $\lambda_n \simeq 0$ for $n \geq L+1$, then the space spanned by $\boldsymbol{e}_n$ for $n \geq L+1$ is called a noise subspace. The MUSIC algorithm uses the characteristic that the transfer function (or Green's function) $\boldsymbol{x}_{\mathrm{true}}$ for the actual delay is orthogonal to the noise subspace as $\boldsymbol{x}_{\mathrm{true}}^{\mathrm{H}}\lambda_n = 0$ for $n \geq L+1$. Hence, a high-resolution signal $f_{\mathrm{MUSIC}}(t)$ can be obtained as

$$f_{\mathrm{MUSIC}}(t) = \frac{\boldsymbol{x}_0(t)^{\mathrm{H}}\boldsymbol{x}_0(t)}{\sum_{n=L+1}^{M} |\boldsymbol{x}_0(t)^{\mathrm{H}}\lambda_n|}, \qquad (6)$$

where $\boldsymbol{x}_0(t)$ is the transfer function assuming an echo with a time delay t.

The actual parameter settings for the MUSIC algorithm for our UWB radar experiment are described below. The MUSIC algorithm is applied in the frequency domain to enhance the resolution for the UWB radar signals as in [2]. First, we select $2M - 1$ frequency-domain data samples with S/N (signal-to-noise ratio) larger than -20 dB, where the maximum power density is 0dB, and $M = 70$ is empirically chosen. Next, a frequency smoothing technique is applied to resolve correlated interferences, where $M \times M$ covariance matrices are averaged M times. Then, an eigenvalue decomposition is applied and a MUSIC spectrum is produced for each antenna location assuming a 2-dimensional signal subspace.

4 Experimental Investigation

Figure 1 shows the experimental UWB radar site in an anechoic chamber. The system includes a short pulse generator, a pair of omni-directional wideband planar patch antennas, and a wideband oscilloscope. The transmitted pulse, with a crassical range resolution of about 50 mm, has a center frequency of 3.7 GHz and bandwidth of 3.0 GHz. In this figure, a 20-mm thick mortar board is set as a target. The distance between the antenna pair and the mortar board is set to 118 mm.

The pulse is transmitted, received by the oscilloscope, converted from analog to digital, and stored in memory. After subtracting the direct wave from the transmitted antenna to the receiving antenna, we obtain the echoes caused by the upper and lower boundaries of the mortar board shown in Fig. 2.
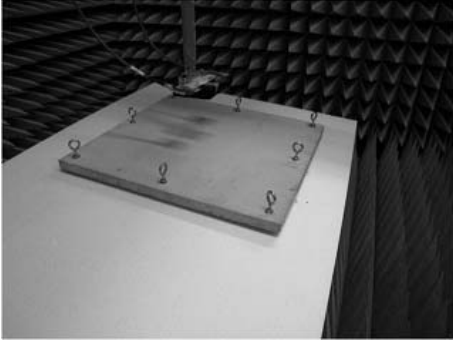
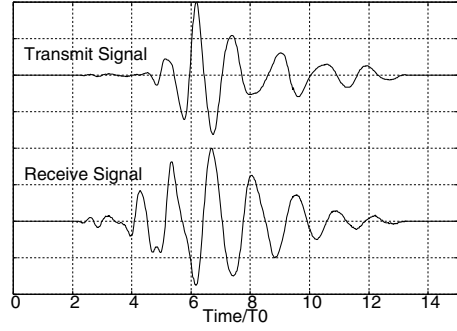Figure 1: Experimental site for UWB radar with a mortar board.

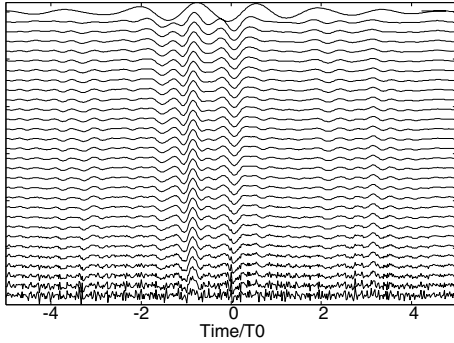Figure 2: Transmitted and received signals with a mortar board.

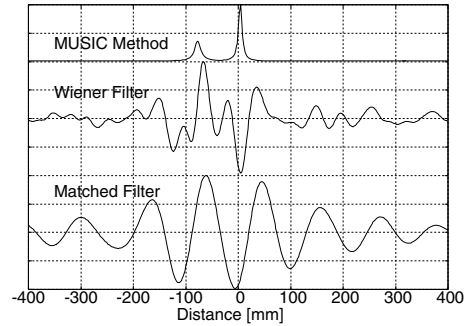Figure 3: High-resolution signal with Wiener filters with various parameters.

Figure 4: Signals processed by MUSIC algorithm, Wiener filter, and matched filter.

A conventional Wiener filter technique is applied to this signal to enhance the resolution

$$F_{\mathrm{W}}(\omega) = F_0(\omega)G^*(\omega)/\{\eta + (1-\eta)|G(\omega)|^2\}, \tag{7}$$

where $0 \leq \eta \leq 1$ is a parameter that depends on the S/N of the signal. Note that the optimal parameter η cannot be determined here because multiple echoes contained in the signal $f(t)$ have different S/N values. Figure 3 shows the output of the Wiener filter for various η applied to the experimental signal from the mortar board, where $\eta = 0$ and $\eta = 1$ correspond to the lower and upper signals, respectively. Although two echoes are seen in this figure, other undesired components are observed as well. Figure 4 shows the signals processed by the MUSIC algorithm, the Wiener filter and the matched filter. Here, an appropriate $\eta = 0.3$ for the Wiener filter is chosen based on the signals in Fig. 3. The output of the matched filter, which has the lowest resolution, cannot resolve the two echoes, whereas the other techniques can resolve them. The resolution of the MUSIC algorithm is much higher than the Wiener filter. Here, the actual number of targets $L = 2$ is given to the MUSIC algorithm. We also set $L = 3$ and 4 to see the output signal and confirm that the image is still clear with a high resolution property, which means that the setting of L does not have much effect on the results.

The relative permittivity of the mortar board is estimated as 4.8 by another measurement. Thus, the equivalent thickness of the board in the UWB radar experiment is calculated as $\sqrt{4.8} \times 2 \times 20\mathrm{mm} = 87.6\mathrm{mm}$. The equivalent thickness estimated from the MUSIC spectrum in Fig. 4 is 82.1 mm which has an error of 5.5 mm or 6.3% of the actual thickness.

Figure 5 shows an experimental setup with part of pig's body as a target. As seen in the figure, the pair of antennas is positioned above the pig's anterior abdominal wall. The two antennas are scanned in a straight line and the received signal is recorded every 5 mm. The pig's anterior abdominal wall is used here as a realistic model of a human body, which is an important study for an attractive application to surveillance and security systems. Figure 6 shows the image obtained by a conventional matched filter. We do not see the detail of the

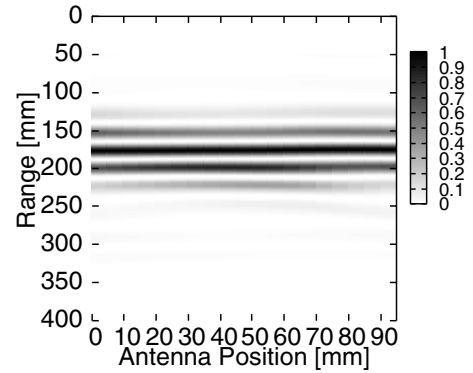Figure 5: Experimental site for UWB radar with an anterior abdominal wall.

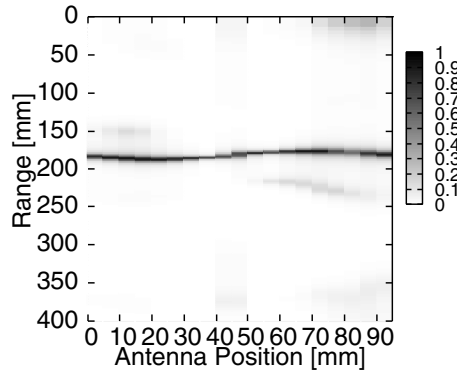Figure 6: Image of the surface of an abdominal wall with the matched filter.

Figure 7: Super-resolution image of the surface of an abdominal wall.

surface fluctuation of the target due to its low resolution property. Figure 7 shows the image estimated with the MUSIC algorithm, in which a clear target boundary is visible with a high resolution of about 10 mm. This is 5 times higher than the classical resolution of 50 mm. This super-resolution technique can be employed in conjunction with the SEABED algorithm to obtain a detailed structure of the human body.

5   Conclusion

In this paper, we investigated experimentally super-resolution techniques for UWB radar data using a mortar board and a pig's anterior abdominal wall as a model of the human body. The results showed that the super-resolution techniques work well to improve the UWB radar performance. The results indicate that it is possible to obtain a high-resolution image within a short time by using a super-resolution technique together with the SEABED algorithm. The investigation of low-computational, high-resolution techniques should be an important future study.

References

[1] T. Sakamoto, IEICE Trans. on Commun., "A fast algorithm for 3-dimensional imaging with UWB pulse radar systems," vol.E90-B, no.3, pp.636-644, Mar. 2007.

[2] C. Le Bastard, V. Baltazart, Y. Wang and J. Saillard, IEEE Trans. on Geosc. & Remote Sensing, vol. 45, no. 8, pp. 2511–2519, 2007.

[3] T. Sakamoto and T. Sato, "Fast imaging of a target in inhomogeneous media for pulse radar systems," Proc. 2004 IEEE International Geoscience and Remote Sensing Symposium vol. 3, pp. 2070–2073, Sep. 2004.

[4] T. Sakamoto and T. Sato, "A fast algorithm of 3-dimensional imaging for pulse radar systems," Proc. 2004 IEEE AP-S International Symposium and USNC/URSI National Radio Science Meeting, vol. 2, pp. 2099–2102, June, 2004.

[5] T. Sakamoto and T. Sato, "A phase compensation algorithm for high-resolution pulse radar systems," IEICE Trans. Communications, vol. E87–B, no. 11, pp. 3314–3321, Nov., 2004.

[6] T. Sakamoto and T. Sato, "A phase compensation algorithm for high-resolution pulse radar systems," Proc. 2004 International Symposium on Antennas and Propagation, pp. 585–588, Aug. 2004.

[7] T. Sakamoto and T. Sato, "A target shape estimation algorithm for pulse radar systems based on boundary scattering transform," IEICE Transaction on Communications vol. E87-B, no. 5, pp. 1357–1365, May 2004.

[8] R. O. Schmidt, "Multiple emitter location and signal parameter estimation," Proc. RADC Spectral Est. Workshop, pp. 243–258, 1979.